Microscopy and Microanalysis (2022), **28**, 1905–1916
doi:10.1017/S1431927622012272

Microscopy AND Microanalysis

Original Article

Energy-Dispersive X-Ray Spectrum Simulation with NIST DTSA-II: Comparing Simulated and Measured Electron-Excited Spectra

Dale E. Newbury* and Nicholas W. M. Ritchie
National Institute of Standards and Technology, Gaithersburg, MD 20899, USA

Abstract

Electron-excited X-ray microanalysis with energy-dispersive spectrometry (EDS) proceeds through the application of the software that extracts characteristic X-ray intensities and performs corrections for the physics of electron and X-ray interactions with matter to achieve quantitative elemental analysis. NIST DTSA-II is an open-access, fully documented, and freely available comprehensive software platform for EDS quantification, measurement optimization, and spectrum simulation. Spectrum simulation with DTSA-II enables the prediction of the EDS spectrum from any target composition for a specified electron dose and for the solid angle and window parameters of the EDS spectrometer. Comparing the absolute intensities for measured and simulated spectra reveals correspondence within ±25% relative to K-shell and L-shell characteristic X-ray peaks in the range of 1–11 keV. The predicted M-shell intensity exceeds the measured value by a factor of 1.4–2.2 in the range 1–3 keV. The X-ray continuum (bremsstrahlung) generally agrees within ±10% over the range of 1–10 keV. Simulated EDS spectra are useful for developing an analytical strategy for challenging problems such as estimating trace detection levels.

Key words: EDS simulation, electron-excited X-ray microanalysis, elemental analysis, energy-dispersive spectrometry (EDS), NIST DTSA-II software

(Received 9 May 2022; accepted 29 June 2022)

Introduction

Some General Observations on Quantitative Electron-Excited X-Ray Microanalysis

Electron-excited X-ray microanalysis performed with a scanning electron microscope (SEM) equipped with energy-dispersive spectrometry (EDS) is a powerful characterization tool that is widely used in materials science and engineering for quantitative elemental analysis spatially resolved at the micrometer to nanometer scale (Goldstein et al., 2018). The microanalyst is supported by comprehensive instrument control software that collects and processes the EDS spectrum to identify elemental constituents in the electron-excited specimen volume and to perform the calculations necessary for quantitative analysis. The electron-excited X-ray spectrum consists of characteristic X-ray peaks superimposed on a background of bremsstrahlung X-rays that form a continuum from the measurement threshold (nominally 100 eV; note some EDS systems can detect X-rays as low in energy as Li K at 52 eV) to the incident beam energy, E_0 (the Duane–Hunt limit). Analysis proceeds by first extracting the characteristic intensity for each peak of interest from the continuum background and eliminating any intensity from interfering peaks of other constituents. The most rigorous degree of quantification is achieved by measuring the characteristic X-ray ("X") intensity, I_{Xi}, for each element, i, in the unknown ("unk") compared to that measured on a standard ("stnd") at the same beam energy and at known dose:

$$k_i = I_{Xi(\mathrm{unk})}/I_{X_{i(\mathrm{stnd})}}. \quad (1)$$

This "k-ratio" of intensities is proportional to the ratio of mass concentrations of unknown to standard:

$$C_{i(\mathrm{unk})}/C_{i(\mathrm{stnd})} \approx k_i. \quad (2)$$

A pure element can serve as a standard, and for those elements that are not solid under vacuum (e.g., O, F, Cl, etc.), are so reactive as to preclude polishing (e.g., Na, K, P, etc.), or which suffer degradation under electron bombardment (e.g., S, etc.), a stable stoichiometric compound can be used (e.g., MgO, SiO_2, CaF_2, KCl, GaP, FeS_2, etc.). The constant of proportionality that can be applied to yield the elemental concentration(s) for the unknown is calculated as a series of "matrix correction (or interelement) factors" that consider the physics of the electron beam and X-ray interactions with matter. These factors arise from differences between the unknown and standard in electron backscattering and energy loss within the target ("Z" factor), in X-ray absorption while propagating through the target in the direction of the EDS ("A" factor), and in the subsequent emission (fluorescence) of additional characteristic X-rays following absorption of electron-induced characteristic and continuum (bremsstrahlung) X-rays in the target ("F" factor for characteristic X-rays and "c" factor for continuum X-rays):

$$C_{i(\mathrm{unk})}/C_{i(\mathrm{stnd})} = k_i/\mathrm{ZAFc}. \quad (3)$$

*Corresponding author: Dale E. Newbury, E-mail: dale.newbury@nist.gov

Cite this article: Newbury DE, Ritchie NWM (2022) Energy-Dispersive X-Ray Spectrum Simulation with NIST DTSA-II: Comparing Simulated and Measured Electron-Excited Spectra. *Microsc Microanal* **28**, 1905–1916. doi:10.1017/S1431927622012272

Rigorous testing of the standards-based/matrix corrections quantification protocol on materials of known composition that are microscopically homogeneous has revealed that 95% of results fall within ±5% relative deviation from the expected value (RDEV), which is defined as:

$$\text{RDEV} = [(\text{measured value} - \text{reference value})/\text{reference value}] \times 100\%, \quad (4)$$

where the measured value is the normalized mass concentration and the reference value is the independently known mass concentration, e.g., a certified reference material (Goldstein et al., 2018).

NIST DTSA-II EDS Software

While comprehensive commercial EDS software is provided to the analyst as part of an SEM-EDS, such software is often considered "company proprietary" so that the details of the procedures for processing spectra and performing quantitative calculations are not publicly revealed. Moreover, without a license, the software is not available to third parties for the universal access to data and analytical procedures that is increasingly required for publication. To meet this need for universal access, "DTSA-II" has been developed by NIST as an open-access, fully documented, and freely available comprehensive software platform for EDS quantification, measurement optimization, and spectrum simulation (Ritchie, 2021). DTSA-II operates on platforms supporting the Java Runtime Environment 16.0 (Windows, Apple, Linux, Unix).

As a quantitative EDS tool that utilizes the standards-based *k*-ratio protocol described above, DTSA-II has been shown to produce high-accuracy results, achieving RDEV values less than ±3% in at least 95% of analyses, when tested against materials of known compositions that have been demonstrated to be homogeneous at the microscopic level (Newbury & Ritchie, 2015*a*). Moreover, accurate results have been obtained with DTSA-II for challenging analytical problems, including situations involving severe peak interference and a large relative concentration ratio of the mutually interfering constituents (Newbury & Ritchie, 2018); low atomic number elements (B, C, N, O, and F) that are subject to large absorption within the target (Newbury & Ritchie, 2015*b*); analysis at a low beam energy of 5 keV or lower (Newbury & Ritchie, 2016*a*); and measurement of trace-level constituents (Newbury & Ritchie, 2016*b*).

DTSA-II includes a comprehensive EDS spectrum simulation mode that can proceed through two different routes, an analytic model and a Monte Carlo electron trajectory simulation, which are constructed using the best available algorithms from the literature (Ritchie, 2009). The analytic simulation, which is restricted to the case of a flat, bulk (i.e., electron opaque) target, utilizes the "$\varphi(\rho z)$" model of Pouchou & Pichoir (1991) for the electron-induced characteristic X-ray production as a function of depth into the specimen. For each depth increment, the generated X-ray intensity is subjected to the appropriate composition-dependent absorption along the path to an EDS spectrometer placed at a known angle relative to the specimen surface ("X-ray take-off angle") to determine the emitted characteristic X-ray intensity. The X-ray bremsstrahlung is calculated following the model of Small et al. (1987) and subjected to the appropriate absorption in the target along the same path to the detector. The emitted characteristic and bremsstrahlung intensities are subjected to further absorption upon passing through the EDS isolation window and detector surface electrode. The broadening that results from the physics of the EDS photon detection process ["resolution function", as defined as a function of photon energy from the full peak width at half peak intensity (FWHM) measured at Mn K–$L_{2,3}$ (Mn Kα)] is then applied to the intensity in each channel to produce the final composite characteristic and bremsstrahlung spectrum.

The Monte Carlo electron trajectory simulation follows the trajectory of a beam electron through the target as it undergoes elastic scattering, which changes the direction of travel. The elastic scattering angle for each event is chosen from the distribution of possible angles by appropriate statistical weighting, and the frequency of elastic scattering is selected by the elastic mean free path, which gives the step length of the trajectory segments. Inelastic scattering is simulated as the continuous energy loss along the step length. At any elastic scattering location, the position coordinates $\{x, y, z\}$ and the velocity components $\{v_x, v_y, v_z\}$ of the electron are known as well as the kinetic energy E_i. Comparison of the position coordinates to the surface(s) of the target enables the determination of backscattering events, and progressive energy loss sets the ultimate travel within the target. The probability of characteristic and bremsstrahlung production along the trajectory segment is calculated and subjected to absorption along the path to the detector to yield the contribution to the emitted spectrum. As in the case for the analytic model, the emitted characteristic and bremsstrahlung X-rays undergo absorption by the detector isolation window and detector electrode and are then subjected to the detector broadening function to yield the final spectrum. The DTSA-II spectrum simulation tool calculates the absolute X-ray intensity in each channel of the spectrum based upon the user-supplied information on the dose (beam current multiplied by EDS live time) and the EDS solid angle (detector area, window support grid open area, and specimen-to-detector distance). The solid angle may be estimated by measuring the sample-to-detector distance and further refined by fine-tuning this distance to produce the best spectral intensity agreement. The calculated channel-by-channel intensity is then subjected to the Poisson distribution to produce the final "noisy" spectrum. An example of the simulated emitted spectrum of GeTe at a beam energy $E_0 = 20$ keV is shown in Figure 1a, where the characteristic X-ray emitted peaks are shown with a width of one channel (5 eV), which is similar to their natural width of a few eV, and with an expanded vertical scale in Figure 1b where the continuum background can be seen and the effect of the applied counting statistics is evident in the channel-to-channel intensity variations. The transformation of this emitted spectrum after EDS detection is shown in Figure 2, where the characteristic peaks have been broadened appropriately to a resolution of 131 eV measured at Mn K–$L_{2,3}$ (Mn Kα).

Because of the fine-scale monitoring of the beam electron position, the Monte Carlo simulation has the flexibility to deal with complex specimen geometries to determine when the beam electron has penetrated through any target surface, including changes of composition at interfaces. DTSA-II includes a number of "set pieces" of specific target geometry for which the user can supply target composition(s) and dimensions through a graphical user interface:

Various bulk target configurations:

1. A flat, bulk homogeneous material
2. A film on a flat, bulk homogeneous material
3. A buried layer in a flat, bulk homogeneous material

https://doi.org/10.1017/S1431927622012272 Published online by Cambridge University Press

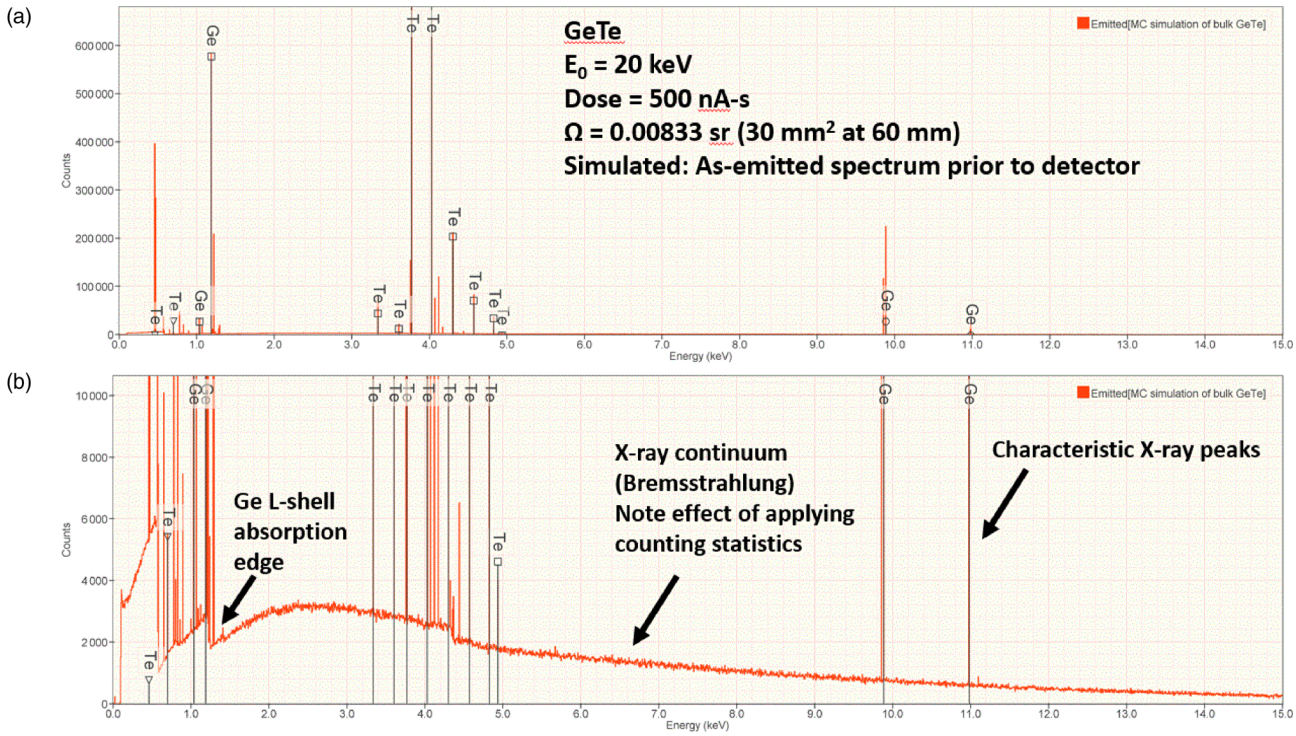

Fig. 1. Simulated EDS spectrum emitted from GeTe at $E_0 = 20$ keV: (**a**) displayed with full intensity range, showing the narrow characteristic X-ray peaks; (**b**) expanded intensity scale showing the bremsstrahlung background.

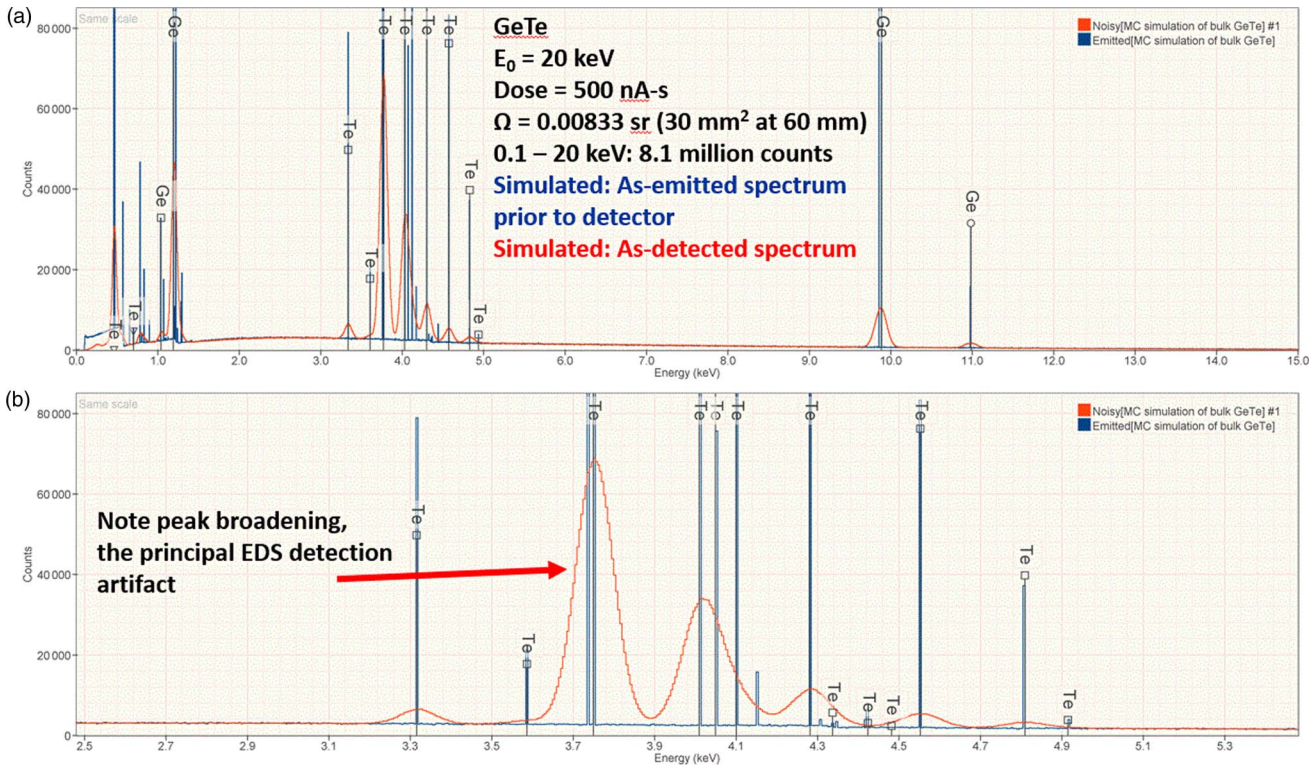

Fig. 2. Simulated EDS spectrum of GeTe at $E_0 = 20$ keV after EDS detection showing the effect of the EDS resolution function broadening the characteristic X-ray peaks: (**a**) spectrum shown for the photon energy range 0–15 keV with full intensity range; (**b**) spectrum shown for the region of the Te L-family peaks with expanded intensity scale.

https://doi.org/10.1017/S1431927622012272 Published online by Cambridge University Press

4. An embedded inclusion (rectangular prism with square base) that intersects the surface of a flat, bulk homogeneous material
5. A beam placed relative to a vertical interface between two materials in a flat bulk target

Various microscopic particle configurations:

1. A sphere placed on a flat, bulk homogeneous material
2. A cube placed on a flat, bulk homogeneous material
3. A rectangular block
4. A hemispherical cap
5. A pyramid with a square base
6. A cylinder on its side
7. A cylinder on its end
8. An equilateral prism

Additionally, the user can script the Monte Carlo code within DTSA-II using a built-in Python-syntax interpreter to devise other target geometries not available in the "set pieces."

For all these simulation modes, the user can invoke the "variable pressure microscopy" option and specify the gas species in the sample chamber, the partial pressure of the gas, and the path length through the gas that the beam must penetrate. Beam electrons are progressively lost from the focused probe due to elastic scattering events with gas atoms leading to the creation of a scattering "skirt" around the focused probe that degrades, often severely, the spatial resolution of the analysis (Goldstein et al., 2018).

Spectrum simulation provides a valuable tool for the analyst because it is generally not possible to have access to a multi-constituent material of arbitrary composition, which is also homogeneous at the microscopic level, that could be used to develop an analytical strategy to address challenging measurement problems. An example would be seeking to establish the measurement conditions needed to achieve a specified limit of detection in a complex material. This work explores spectrum simulation with DTSA-II, examining how well the simulated spectra compare to spectra measured from known materials under defined dose and detector solid angle conditions.

Materials and Methods

Materials examined in this study included pure elements and stoichiometric compounds procured from commercial vendors. Multi-constituent materials included NIST Standard Reference Materials (SRM) and Research Materials (RM) specifically created to satisfy the requirement of homogeneity on a microscopic scale to serve as microanalysis test materials of the independently determined bulk composition.

Electron-excited X-ray spectrometry was performed using the JEOL 8,500 F thermal field emission electron probe microanalyzer. Over the period of these measurements, two different EDS systems were used: (1) a Bruker QUAD system with four 10 mm^2 silicon drift detectors at a 72 mm specimen-to-detector distance and (2) a Bruker Quantax XFlash single 30 mm^2 silicon drift detector at a 60 mm specimen-to-detector distance.

EDS spectra were collected using Bruker Esprit software and exported in the ISO/EMSA standard (ISO, 2003) spectral format for subsequent processing with the NIST DTSA-II software for comparison to simulated spectra (Ritchie, 2021). For each measurement condition in this study, a sufficient electron dose was utilized so that the total spectrum count, integrated from a threshold of 0.1 keV to the incident beam energy, E_0, generally exceeded 5 million counts.

EDS spectra were simulated with the DTSA-II Monte Carlo procedure for the bulk, homogeneous material case (Ritchie, 2021). At least 6,000 trajectories were calculated for each condition simulated in this study. Simulated spectra were then compared to measured spectra by using the functions within DTSA-II that integrate intensities over user-defined regions-of-interest, including the "peak—background" tool which measures the characteristic X-ray peak intensity above the bremsstrahlung background.

Results

DTSA-II spectral simulations were performed for an extensive set of pure elements, binary stoichiometric compounds, SRMs, RMs, and alloys. Selected examples for several binary materials comparing the simulated spectrum to the measured spectrum are presented below:

GeTe

Continuing the example of GeTe at $E_0 = 20$ keV from Figures 1 and 2, the measured and DTSA-II simulated EDS spectra are compared in Figure 3. Selected numerical values for the ratio of the Monte Carlo simulation to the experiment spectrum ("MC/EXP") are shown in Figure 3, including the major characteristic X-ray peaks and continuum (bremsstrahlung) windows selected to avoid characteristic peaks and detector artifacts (e.g., escape peaks, coincidence peaks): Ge K–$L_{2,3}$ (Ge Kα) MC/EXP = 1.02; Ge $L_{2,3}$–$M_{4,5}$ (Ge Lα,β) MC/EXP = 0.915; Te L_3–$M_{4,5}$ (Te Lα) MC/EXP = 1.08; Te M-family MC/EXP = 3.53. For the continuum regions selected, the deviation between the simulated and measured intensities was 1.06 or less.

FeS_2

Simulated and measured EDS spectra for FeS_2 at $E_0 = 20$ keV are shown in Figure 4 with selected numerical comparisons listed: S K–$L_{2,3}$–$M_{2,3}$ (S Kαβ) MC/EXP = 1.15; Fe K–$L_{2,3}$ (Fe Kα) MC/EXP = 1.07; Fe $L_{2,3}$–$M_{4,5}$ (Fe Lα,β) MC/EXP = 1.02. For the continuum regions selected, the deviation between the simulated and measured intensities ranges from 0.938 to 1.08.

SRM 482: 60Au–40Cu Alloy

Simulated and measured EDS spectra for NIST Standard Reference Material (SRM) 482:60Au–40Cu alloy at $E_0 = 20$ keV are shown in Figure 5 with selected numerical comparisons listed for K-shell, L-shell, and M-shell peaks: Cu K–$L_{2,3}$ (Cu Kα) MC/EXP = 1.05; Cu L-family MC/EXP = 0.757; Au L_3–$M_{4,5}$ (Au Lα) MC/EXP = 1.09; Au M4,5-N6,7 (Au Mα,β) MC/EXP = 1.45. Selected regions of the continuum from 1 to 10 keV show a range of MC/EXP from 0.97 to 1.08.

PbSe

PbSe provides another example of K-shell, L-shell, and M-shell characteristic X-rays in the same spectrum. Simulated and measured EDS spectra for PbSe at $E_0 = 20$ keV are shown in Figure 6 with selected numerical comparisons listed: Se K–$L_{2,3}$

https://doi.org/10.1017/S1431927622012272 Published online by Cambridge University Press

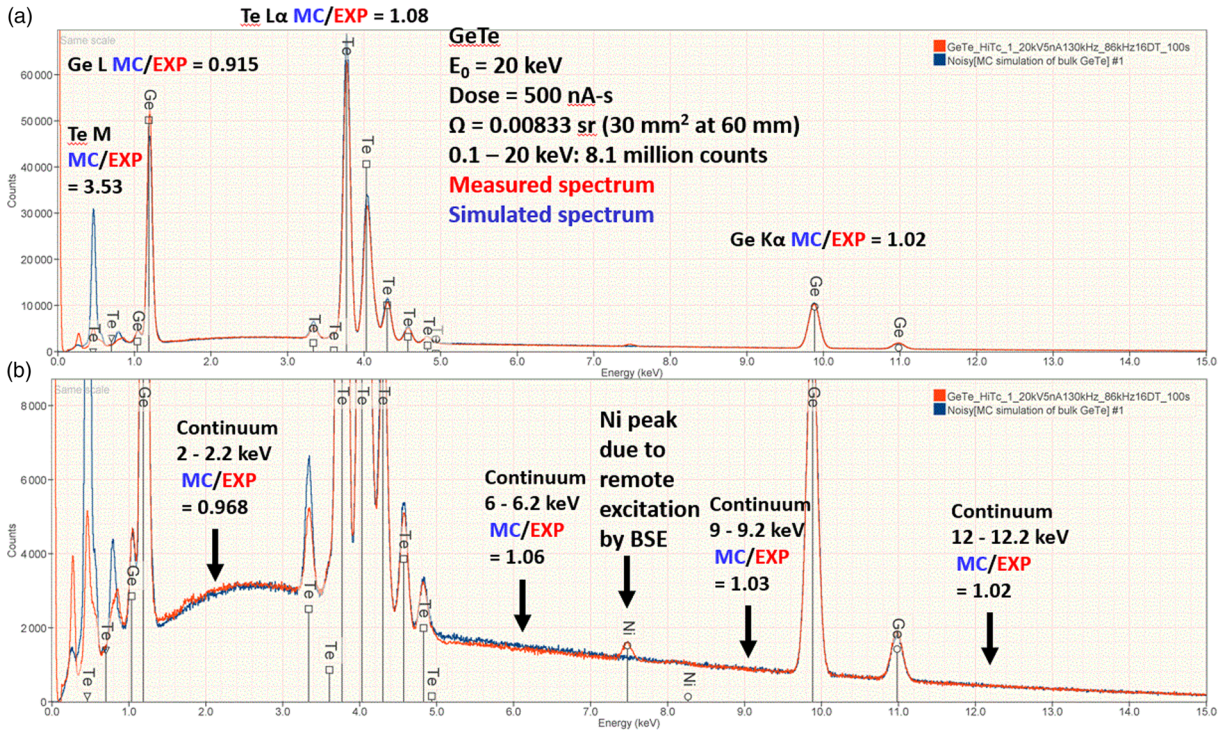

Fig. 3. (**a**) Comparison of the simulated and measured EDS spectra of GeTe at $E_0 = 20$ keV with the intensity ratio Monte Carlo/experimental ("MC/EXP") shown for the principal characteristic X-ray peaks; (**b**) expanded intensity scale showing comparison MC/EXP of the bremsstrahlung X-ray intensity in selected energy regions.

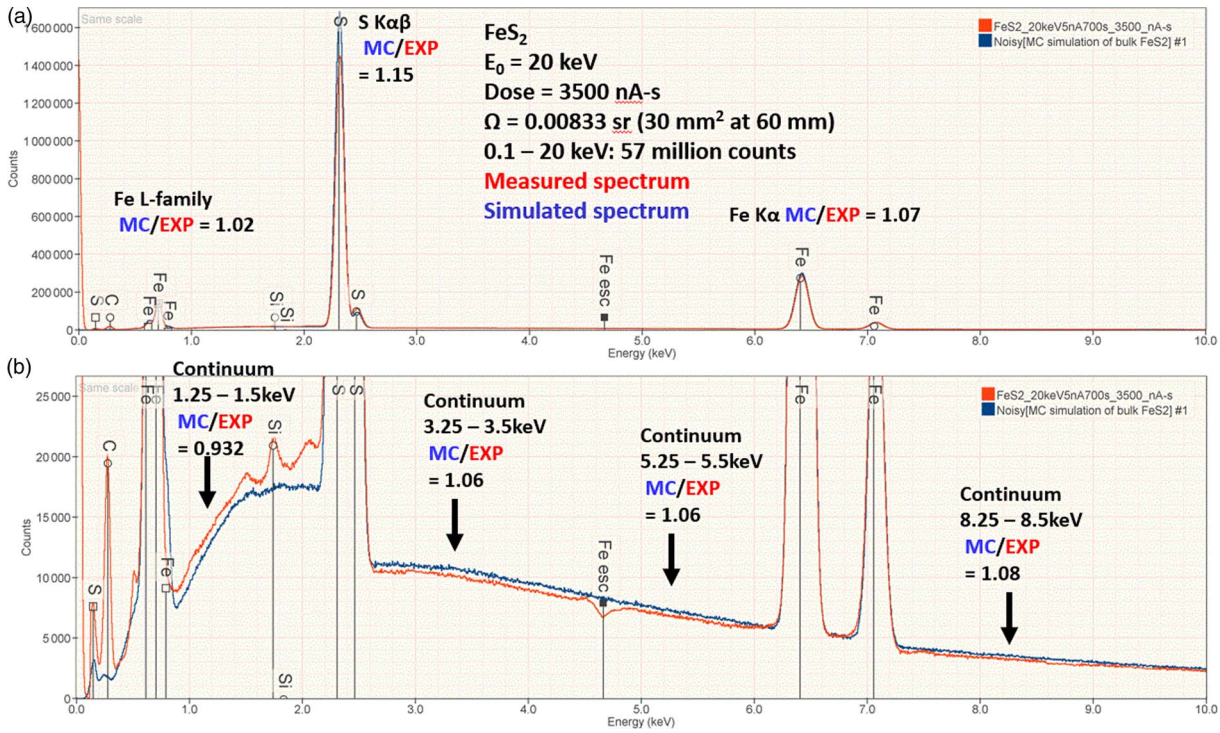

Fig. 4. (**a**) Comparison of the simulated and measured EDS spectra of FeS_2 at $E_0 = 20$ keV with the intensity ratio Monte Carlo/experimental ("MC/EXP") shown for the principal characteristic X-ray peaks; (**b**) expanded intensity scale showing comparison MC/EXP of the bremsstrahlung X-ray intensity in selected energy regions.

(Se Kα) MC/EXP = 1.03; Se $L_{2,3}$–$M_{4,5}$ (Se Lα,β) MC/EXP = 1.11; Pb L_3–$M_{4,5}$ (Pb Lα) MC/EXP = 1.05; Pb M4,5-N6,7 (Pb Mα,β) MC/EXP = 1.44. Selected regions of the continuum show a range of MC/EXP from 1.07 to 1.12.

Comprehensive Comparison of Simulated and Measured Intensities

Figures 7 and 8 present plots of the ratio of the simulated-to-measured absolute intensities for K- and L-shell X-rays in the

https://doi.org/10.1017/S1431927622012272 Published online by Cambridge University Press

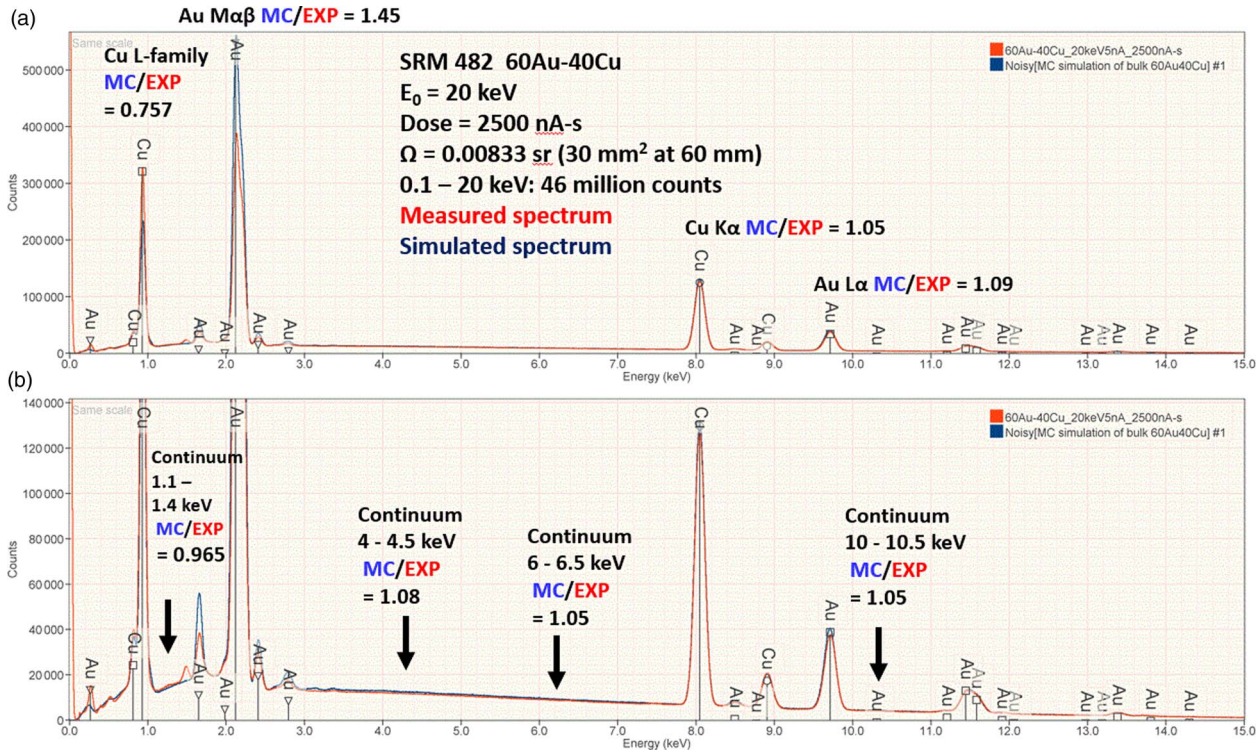

Fig. 5. (**a**) Comparison of the simulated and measured EDS spectra of SRM 482: 60Au–40Cu alloy at $E_0 = 20$ keV with the intensity ratio Monte Carlo/experimental ("MC/EXP") shown for the principal characteristic X-ray peaks; (**b**) expanded intensity scale showing comparison MC/EXP of the bremsstrahlung X-ray intensity in selected energy regions.

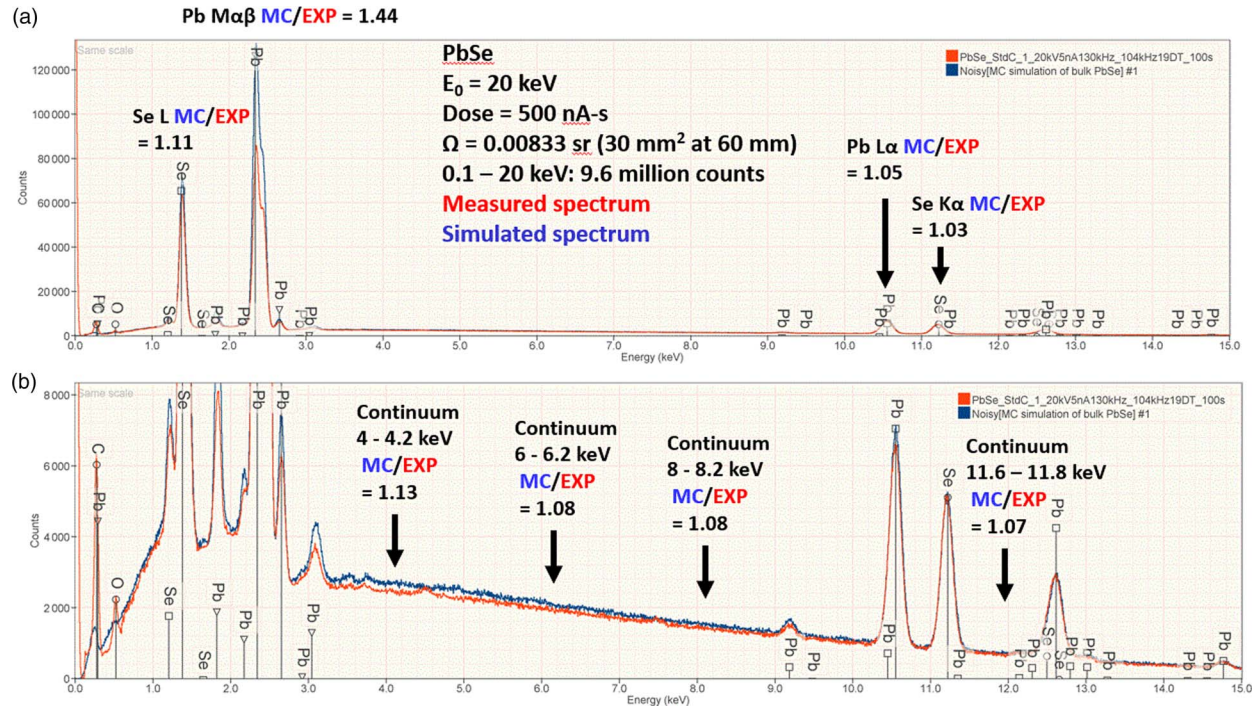

Fig. 6. (**a**) Comparison of the simulated and measured EDS spectra of PbSe at $E_0 = 20$ keV with the intensity ratio Monte Carlo/experimental ("MC/EXP") shown for the principal characteristic X-ray peaks; (**b**) expanded intensity scale showing comparison MC/EXP of the bremsstrahlung X-ray intensity in selected energy regions.

range from 1 to 12 keV at $E_0 = 20$ keV from pure elements and stochiometric compounds. For the K- and L-shells, the agreement is generally within ±25% relative. For the M-shell characteristic X-rays in the energy range from 1 to 3 keV shown in Figure 9, a larger deviation is observed, with the simulated intensity exceeding the experimental measurement by a factor ranging from 1.4 to 2.2.

https://doi.org/10.1017/S1431927622012272 Published online by Cambridge University Press

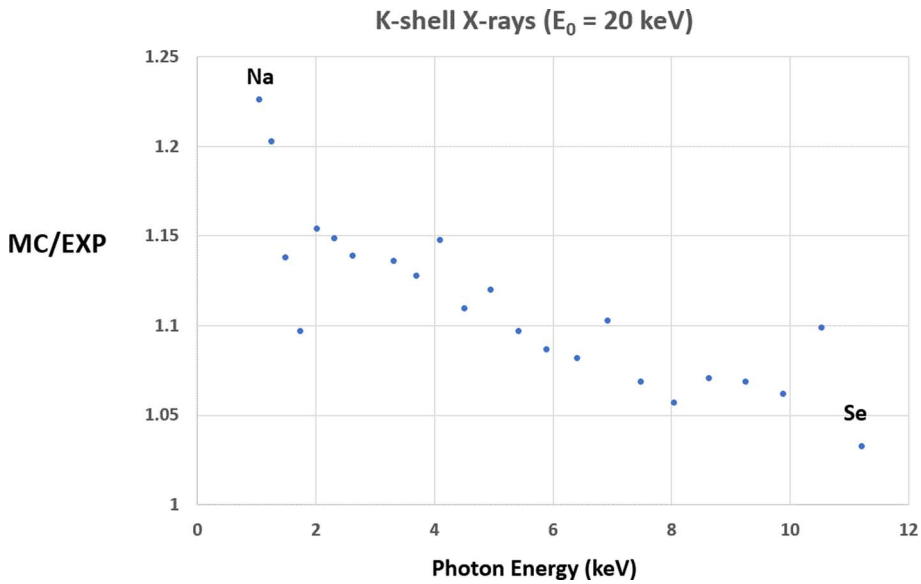

Fig. 7. Monte Carlo simulated to experimentally measured (MC/EXP) absolute intensities for K-shell characteristic X-rays.

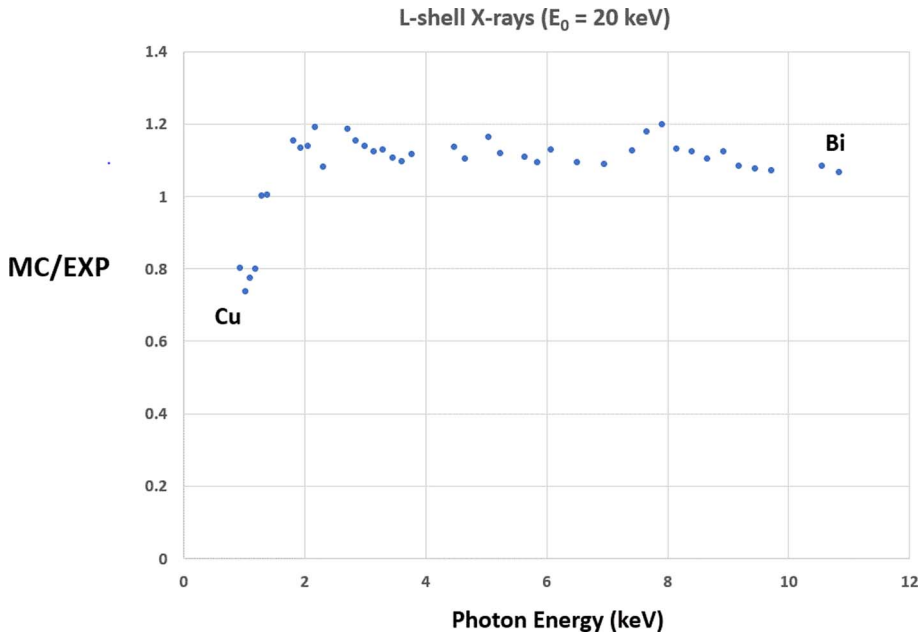

Fig. 8. Monte Carlo simulated to experimentally measured (MC/EXP) absolute intensities for L-shell characteristic X-rays.

In Figure 10, for bremsstrahlung X-rays measured in various energy bands, the agreement is generally within ±10% relative over the full range of elements tested.

Discussion

The deviation between the simulated and measured spectra can arise from several sources:

Measured spectra

1. Uncertainty in the detector solid angle arises from several sources: the detector-to-source distance; the active area of the EDS; and the transmission area of the grid that supports the vacuum isolation window.
2. Uncertainty in the beam current. While the beam current measurement system integrated into the electron beam instrument can provide the repeatable setting of the beam current, the absolute accuracy of this value has uncertainty.

Simulated spectra

1. Uncertainty in the physical parameters for the generation of characteristic and bremsstrahlung X-rays, including the ionization cross section, the fluorescence yield, and other parameters.
2. Uncertainty in the X-ray mass absorption coefficients is needed to accurately determine X-ray absorption loss during propagation from the generation location within the target to the surface in the direction of the EDS.

It is worthwhile to observe that, in a manner similar to standards-based quantification of measured spectra, some of these parameters cancel when both a simulated standard and unknown are used. For

https://doi.org/10.1017/S1431927622012272 Published online by Cambridge University Press

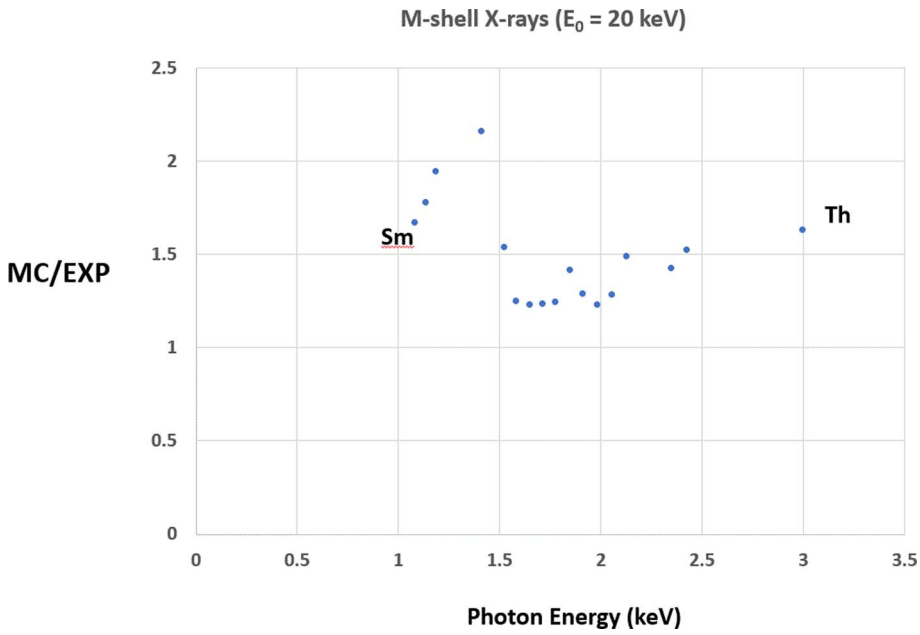

Fig. 9. Monte Carlo simulated to experimentally measured (MC/EXP) absolute intensities for M-shell characteristic X-rays.

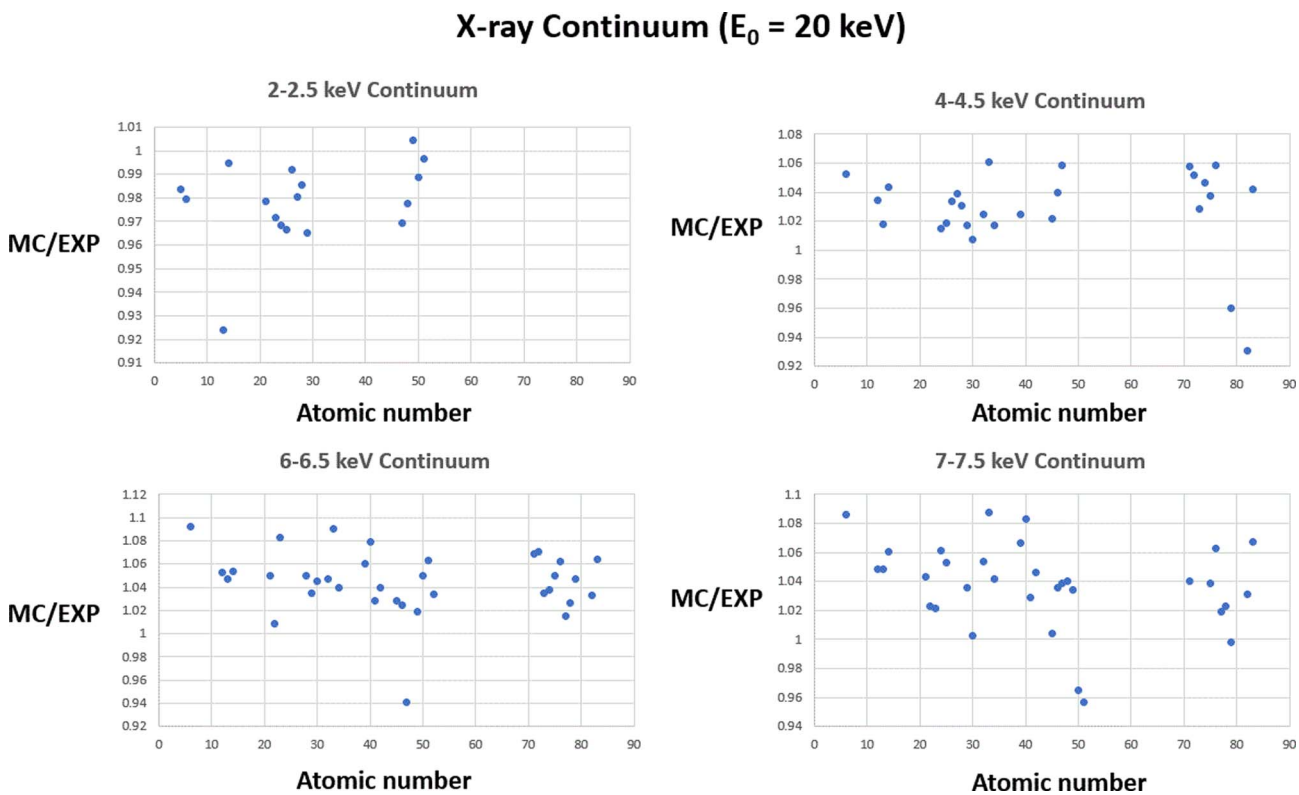

Fig. 10. Monte Carlo simulated to experimentally measured (MC/EXP) absolute intensities for continuum (bremsstrahlung) X-rays in several energy bands.

example, the ionization cross-section and relaxation rates are largely a function of the element and particular transition. It does not depend on the differences in material properties between the standard and the unknown. Thus, a relatively large error in the ionization cross-section or relaxation rate may not be relevant when comparing measured *k*-ratios with simulated *k*-ratios. Likewise for other parameters that are dependent only on the characteristic X-ray's source element. However, properties like the electron scattering cross-section and mass absorption coefficients are properties of the material and will differ between standard and unknown. Because of fortuitous cancelation, it is possible to simulate *k*-ratios with much higher accuracy than raw intensities. An example is presented in Table 1 for the case of SRM 482: 60Au-40Cu alloy, which compares the k-ratios relative to pure element standards for various peaks as determined with DTSA-II for measured and simulated spectra. Thus, while the simulated

https://doi.org/10.1017/S1431927622012272 Published online by Cambridge University Press

Table 1. Comparison of *k*-Ratios Determined from Monte Carlo Simulated EDS spectra and from Experimentally Measured Spectra.

X-Ray Peak	Intensity Ratio MC/EXP	*k*-Ratio Monte Carlo	*k*-Ratio experimental	*k*(MC)/*k*(EXP)
Cu L-family	0.757	0.2663	0.2728	0.9762
Au M4,5-N6,7 (Au Mα,β)	1.45	0.4860	0.4931	0.9856
Cu K–$L_{2,3}$ (Cu Kα)	1.05	0.4515	0.4577	0.9865
Au L_3–$M_{4,5}$ (Au Lα)	1.09	0.5232	0.5261	0.9945

Values are the mean of five replicate measured and simulated spectra.

absolute intensity exceeds the measured intensity by a factor of 1.45 for the Au M4,5-N6,7 (Au Mα,β), the value of *k*(MC)/*k*(EXP) is 0.9856. Similarly, for the Cu L-family, the simulated absolute intensity is 0.757 of the measured intensity, while *k*(MC)/*k*(EXP) is 0.9762. In fact, matrix correction algorithms suffer from a similar dependency on physical parameters. The extent to which Monte Carlo simulation is better at determining the true shape of the $\phi(\rho z)$ curve is the extent to which Monte Carlo-generated *k*-ratios are likely to be better than analytical models. However, this is hard to demonstrate experimentally.

Using DTSA-II Simulated spectra to aid Microanalysis

Simulating spectra with DTSA-II can be an aid to the analyst seeking to develop a strategy to solve a particular problem, such as achieving a required limit of detection. When developing an effective analytical strategy (e.g., choice of beam energy, dose, etc.), the analyst generally does not have access to a known material with an arbitrary composition of interest that is also homogeneous on a microscopic scale, a key requirement for microanalysis. Moreover, nearly all of the limited set of available microanalysis SRMs are certified only for major constituents ($C > 0.1$ mass concentration). When a measurement problem involves minor ($0.01 \leq C \leq 0.1$) or trace constituents ($C < 0.01$), virtually no suitable SRMs are available for test measurements, and spectrum simulation may be the only path forward.

As an example, consider the problem of examining the limits of detection of trace Ca in $SrTiO_3$. Figure 11a shows the simulated spectrum (with dose-appropriate counting statistics applied) at $E_0 = 20$ keV for Ca at 0.001 mass concentration with a dose that produces an integrated total spectrum intensity (0.1 keV to E_0) of 13.8 million counts. The peak for Ca K–$L_{2,3}$ (Ca Kα) is readily apparent by visual inspection. Even with the dose lowered by a factor of 10, the trace Ca peak remains visible, as shown in Figure 11b. In Figure 12a, lowering the concentration of Ca to 0.0002 mass concentration at the dose that produces 13.8 million counts results in a barely noticeable Ca K–$L_{2,3}$ (Ca Kα) peak. Lowering the dose by a factor of 10 in Figure 12b increases the statistical noise to the point where the trace Ca peak is overwhelmed. Although difficult to perceive by visual inspection against the statistical variance in the bremsstrahlung background, a low relative intensity peak from a trace constituent may be recoverable with peak fitting. Quantitative detection of trace constituents can be explored by simulating the spectra of the appropriate standards suite, e.g., Ca (CaF_2), O (MgO), Ti (Ti), and Sr (SrF_2), necessary to "quantify" the simulated trace Ca in $SrTiO_3$ spectrum by using DTSA-II to apply the "standards-based protocol" described in the Introduction section. Results of such a procedure are presented in Table 2 for trace Ca at 0.001 and 0.0002 mass concentration with three different doses. As characterized with the RDEV value, the mean concentration determined for

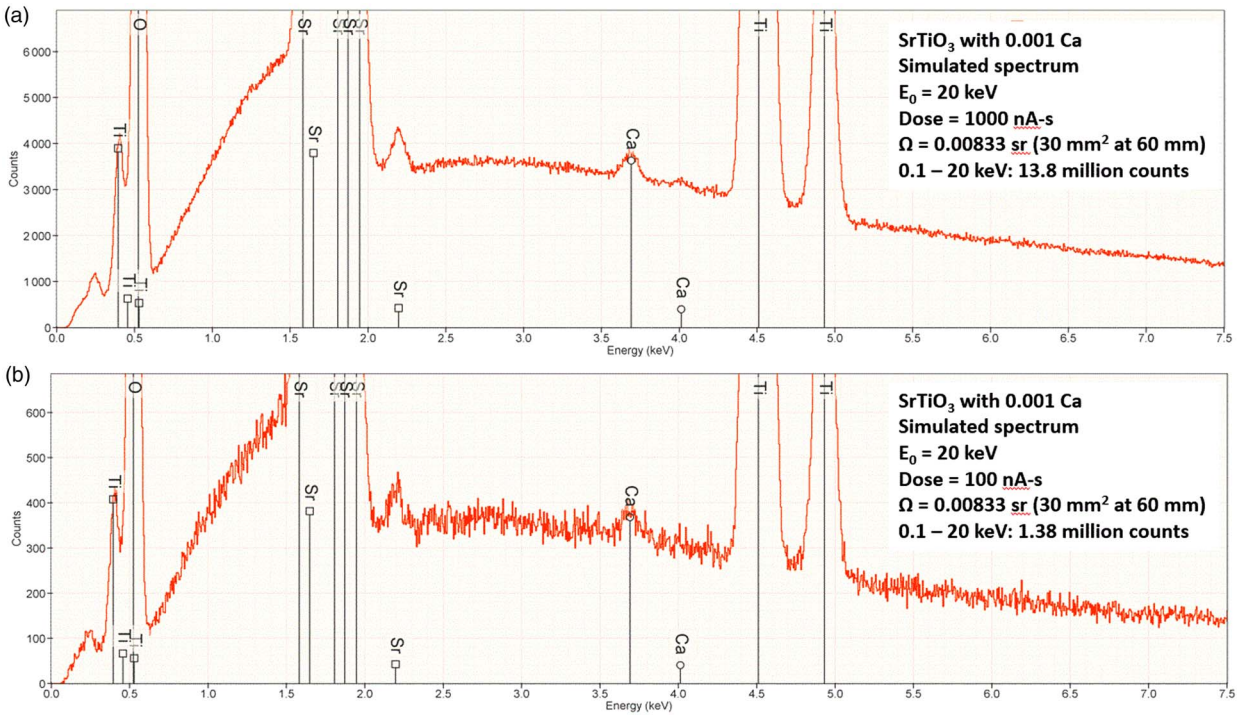

Fig. 11. (**a**) Simulated EDS spectrum of $SrTiO_3$ with trace Ca (0.001 mass fraction) at $E_0 = 20$ keV for a dose that yields 13.8 million counts from 0.1 keV to E_0. (**b**) The effect of lowering the dose to give 1.38 million counts.

https://doi.org/10.1017/S1431927622012272 Published online by Cambridge University Press

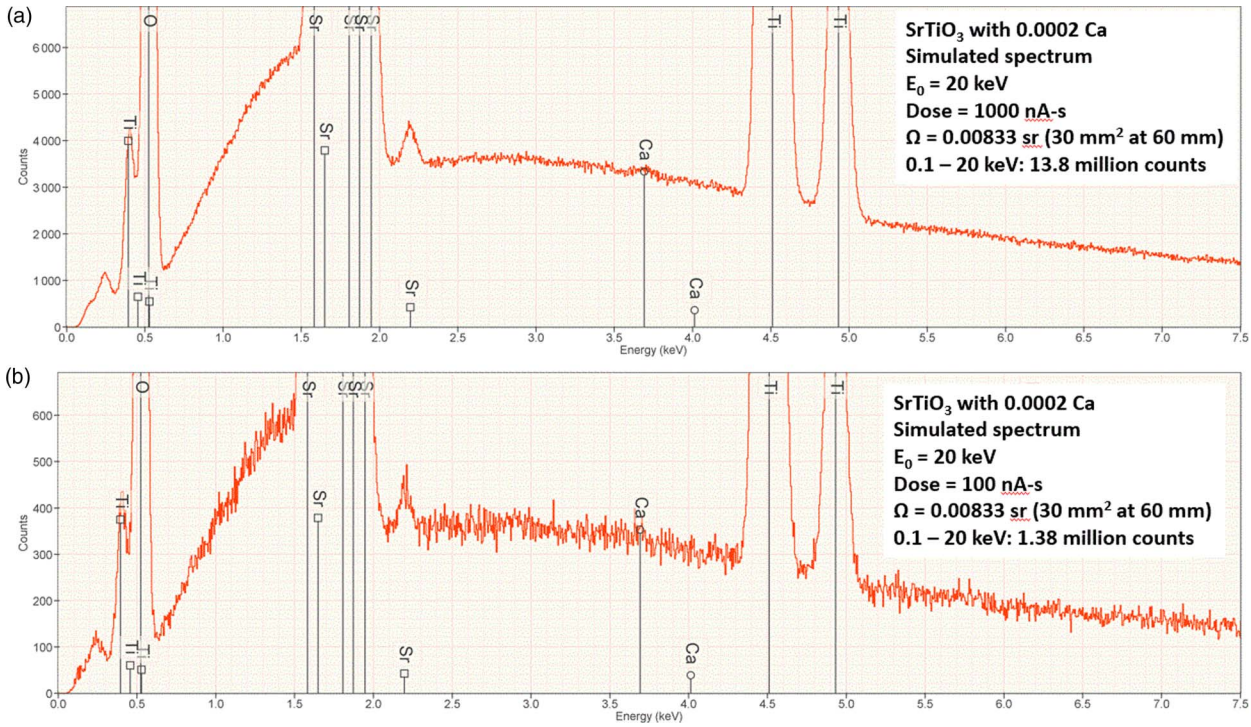

Fig. 12. (**a**) Simulated EDS spectrum of $SrTiO_3$ with trace Ca (0.0002 mass fraction) at $E_0 = 20$ keV for a dose that yields 13.8 million counts from 0.1 keV to E_0. (**b**) The effect of lowering the dose to give 1.38 million counts.

10 replicates for Ca at 0.001 agrees well with the simulated value for all three dose levels. The range of maximum to minimum values within the set of 10 replicates increases as the dose is lowered and at the lowest dose ranges from 0.000907 (RDEV = −9%) to 0.00139 (RDEV = 39%). When the Ca concentration level is lowered to 0.0002 mass concentration, the mean concentration of the 10 replicates at the lowest dose gives an RDEV of 5%, which appears satisfactory, but the maximum to minimum values range from 0.000467 (RDEV = 134%) to 0.0000438 (RDEV = −78%), indicating that single measurements will be unreliable and a higher dose will be necessary to obtain a more robust result.

Assessing Artifacts in Measured EDS spectra

Spectra simulated with DTSA-II include the major artifact of EDS detection which is the peak broadening that results from the physics of the photon-to-charge conversion that occurs in the semiconductor detector. This effect is illustrated in the simulated spectrum of GeTe Figure 2 after emission from the target, which shows narrow characteristic X-ray peaks, and after detection, which shows much broader peaks. There are other artifacts of the EDS detection process that can be revealed by comparing simulated and measured spectra. Figure 13 shows an example of simulated and measured spectra of FeS_2 where incomplete charge collection is revealed as a broadening distortion on the low-energy shoulder of the S K-family. Coincidence features, which occur when two photons arrive in the detector so close in time that they are not recognized as two events by the EDS pulse pile-up rejection function, are observed from various peak combinations: Fe L + S K; S K + S K. It is important to recognize these coincidence artifacts, which might otherwise be misidentified as peaks of legitimate minor or trace-level constituents. An example of a minor/trace peak of Si is revealed in Figure 13.

Table 2. Results of DTSA-II Quantitative Analysis of Simulated spectra of $SrTiO_3$ with Trace Ca Using Simulated Standards (MgO, CaF_2, Ti, and SrF_2).

Ca Conc. Simulated	0.1–20 keV Spectrum Integral (Counts)	Mean Conc. (10 Replicates)	RDEV (%)	Maximum Conc in 10 Replicates	Minimum Conc in 10 Replicates	σ (10 Replicates)	$\sigma_{relative}$ (10 Replicates) (%)
0.001	1.38 million	0.00105	5	0.00139	0.000907	0.000141	13.4
0.001	13.8 million	0.000988	−1.2	0.00106	0.000892	0.000055	5.6
0.001	138 million	0.00102	2	0.00104	0.000995	0.000014	1.4
0.0002	1.38 million	0.000210	5	0.000467	0.0000473	0.000134	64
0.0002	13.8 million	0.000177	−11	0.000231	0.000105	0.0000438	25
0.0002	138 million	0.000192	−4	0.000213	0.000172	0.0000127	6.6
Blank	138 million	0.000015	NA	0.000026	0.000002	0.0000068	45

https://doi.org/10.1017/S1431927622012272 Published online by Cambridge University Press

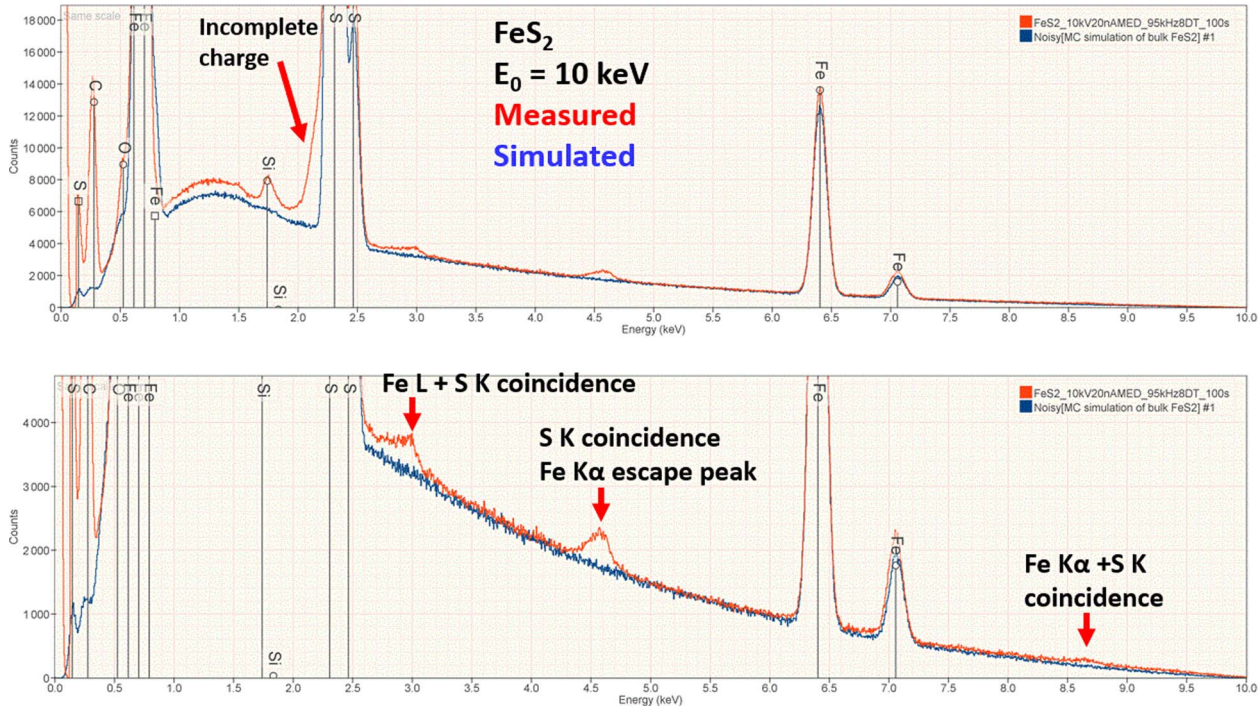

Fig. 13. Simulated and measured EDS spectra of FeS_2 at $E_0 = 10$ keV. Note the artifacts arising from incomplete charge collection on the low-energy shoulder of the S K-family and the various coincidence peaks.

Considering the example of simulating trace Ca in $SrTiO_3$, the possible occurrence of coincidence peaks from the Si L-family in the region of the Ca K-family must be considered. Comparing the simulated spectrum of $SrTiO_3$ with a measured spectrum in Figure 14 reveals a nearby anomalous peak structure centered at 3.6 keV that arises from Sr L_3–$M_{4,5}$ (Sr Lα) coincidence, which may interfere with the measurement of trace Ca. Such a coincidence peak(s) could be reduced by lowering the beam current and thus the system deadtime, but such a measurement strategy would have to also include a longer counting time to accumulate adequate counts to achieve the desired limit of detection for the element(s) of interest.

Summary

NIST DTSA-II provides the microanalyst with software tools to analyze and simulate electron-excited EDS X-ray spectra. The correspondence of the absolute intensity between measured and simulated spectra is generally within ±25% for K-shell and L-shell characteristic X-rays in the energy range from 1 to 11 keV. For M-shell characteristic X-rays in the energy range from 1 to 3 keV, the simulated intensity exceeds the measured intensity by a factor of 1.4–2.2. The continuum (bremsstrahlung) intensity generally agrees within ±10% relative. It is generally possible to simulate *k*-ratios with much higher accuracy than raw intensities. Spectra simulated with DTSA-II can be used to develop an

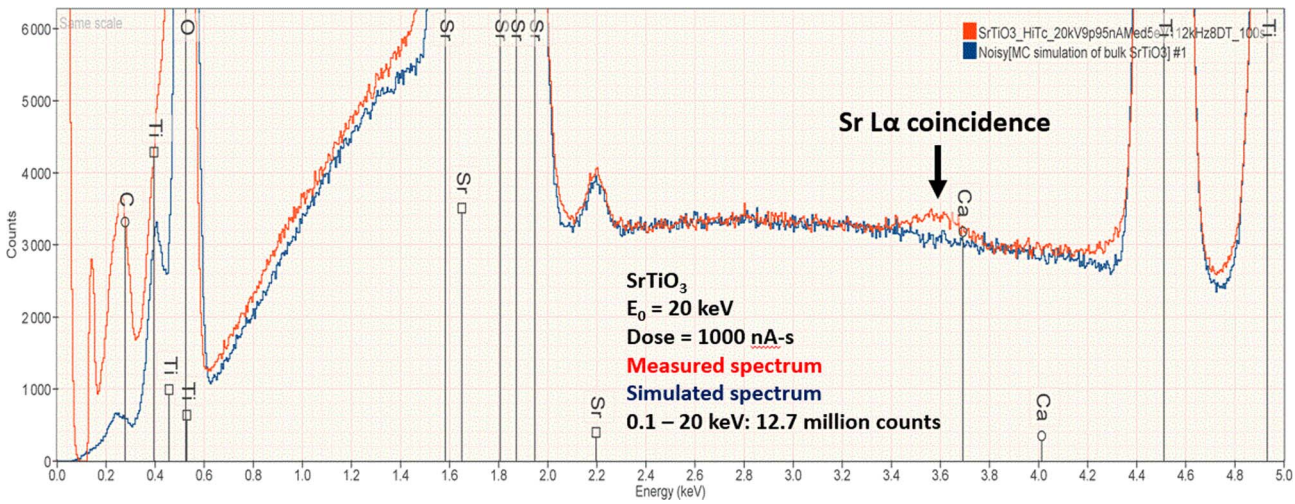

Fig. 14. Simulated and measured EDS spectra of $SrTiO_3$ at $E_0 = 20$ keV. Note the artifact arising from the Sr L_3–$M_{4,5}$ (Sr Lα) coincidence.

https://doi.org/10.1017/S1431927622012272 Published online by Cambridge University Press

analytical strategy, such as estimating the dose needed to detect and quantify minor and trace constituents in a putative target composition. Simulated spectra compared with measured spectra can reveal the presence of artifacts in the measured spectra.

Acknowledgments. This work was undertaken as part of the authors' official duties as employees of the National Institute of Standards and Technology, an agency of the United States Department of Commerce.

Conflict of interest. The authors certify that they have no competing interests that could impact any aspect of this work, which was undertaken as part of their official duties as employees of the National Institute of Standards and Technology, an agency of the United States Department of Commerce.

NIST disclaimer. Certain commercial equipment, instruments, or materials are identified in this paper to foster understanding. Such identification does not imply recommendation or endorsement by the National Institute of Standards and Technology, nor does it imply that the materials or equipment identified are necessarily the best available for the purpose.

References

Goldstein J, Newbury D, Michael J, Ritchie N, Scott J & Joy D (2018). *Scanning Electron Microscopy and X-Ray Microanalysis*, 4th ed. New York: Springer.

International Organization for Standardization (2003). standard ISO 22029:2003.

Newbury D & Ritchie N (2015*a*). Review: Performing elemental microanalysis with high accuracy and high precision by scanning electron microscopy/silicon drift detector energy dispersive X-ray spectrometry (SEM/SDD-EDS). *J Mats Sci* **50**, 493–518.

Newbury DE & Ritchie NWM (2015*b*). Quantitative electron-excited X-Ray microanalysis of borides, carbides, nitrides, oxides, and fluorides with scanning electron microscopy/silicon drift detector energy-dispersive spectrometry (SEM/SDD-EDS) and DTSA-II. *Microsc Microanal* **21**(2015), 1327–1340.

Newbury DE & Ritchie NWM (2016*a*). Electron-excited X-ray microanalysis at low beam energy: Almost always an adventure!. *Micros Microanal* **22**, 735–753.

Newbury DE & Ritchie NWM (2016*b*). Measurement of trace constituents by electron-excited X-ray microanalysis with energy-dispersive spectrometry. *Microsc Microanal* **22**, 520–535.

Newbury DE & Ritchie NWM (2018). An iterative qualitative–quantitative sequential analysis strategy for electron-excited X-ray microanalysis with energy dispersive spectrometry: Finding the unexpected needles in the peak overlap haystack. *Microsc Microanal* **24**, 350–373.

Pouchou J-L & Pichoir F (1991). Quantitative analysis of homogeneous or stratified microvolumes applying the model "PAP. In *Electron Probe Quantitation*, Heinrich KFJ & Newbury DE (Eds.), pp. 31. New York: Plenum.

Ritchie NW (2021). DTSA-II open access software for quantitative electron excited X-ray microanalysis with energy dispersive spectrometry. available for free, including tutorials, at the NIST. Available at https://www.nist.gov/services-resources/software/nist-dtsa-ii

Ritchie NWM (2009). Spectrum simulation in DTSA-II. *Microsc Microanal* **15**, 454–468.

Small JA, Leigh SD, Newbury DE & Myklebust RL (1987). Modeling of the bremsstrahlung radiation produced in pure-element targets by 10–40 keV electrons. *J Appl Phys* **61**, 459–469.

https://doi.org/10.1017/S1431927622012272 Published online by Cambridge University Press